Ab initio band structure of quasi-metallic carbon nanotubes for terahertz applications

P N D'yachkov, I A Bochkov

Institute of General and Inorganic Chemistry, Russian Academy of Sciences, Leninskii Pr. 31, Moscow 119991, Russia

Corresponding author's e-mail: p_dyachkov@rambler.ru

Abstract

Two integers (n_1, n_2) determine the band structure of single-walled carbon nanotubes (CNTs). According to π-electron zone-folding model, an energy gap between the valence and conduction bands disappears if a difference $n_1 - n_2 = 3q$ is divisible by three. Such CNTs are called the quasi-metallic tubules. An account of surface curvature of tubules predicts that a small gap opens in such CNTs and they are the narrow-gap semiconductors really. Available experimental and theoretical information on the gap energies is very limited. In this paper, the band structures of the 50 CNTs (n_1, n_2) with $4 \le n_1 \le 18$ and $n_2 = n_1 - 3q$ are calculated using a linearized augmented cylindrical waves method. The quasi-metallic CNTs with optical gaps falling within the terahertz range (1 - 40 meV) are identified, which can be used to design the high-frequency devices like the terahertz emitters, detectors, multipliers, antennas, polarizers, and transistors.

1 Introduction

Single-walled carbon nanotubes (CNTs) are the giant molecules looking like the closed hollow cylinders with carbon hexagons tiling on the surface. There is a close link between the geometry and band structure of graphene and nanotubes. The geometry of any CNT can be thought of as a result of rolling up a graphene ribbon into a seamless cylinder and can be characterized by the two positive integers (n_1, n_2) defining the way in which it is rolled. Neglecting the nanotubes surface

curvature, the important features of the π-electron band structure of the nanotubes were obtained in the terms of simple zone-folding model of graphene π-bands [1 - 5]. This approximation shows that there is an overlap of π-bands in the Fermi level region in the case of (n,n) CNTs and these tubules have the metallic-type band structures; the (n_1, n_2) CNTs with $n_1 - n_2$ indivisible by three are the semiconductors having a few tenths of eV energy gaps. Finally, if $n_1 - n_2 = 3q$ (q = 1, 2, …), the tubules should have the semi-metallic band structure with zero energy gap between valence and conduction bands; however, beyond the π-electron zone-folding model, an account of tubules curvature predicts that the small gaps equal to about $1 - 100$ meV open [6 - 10]. Often, these nanotubes are called the quasi-metallic tubules; they are the narrow-gap semiconductors really. These gaps were detected experimentally using the atomically resolved scanning tunnel microscopy [11], optical transmission spectroscopy [12 - 14], and by performing optical and electrical measurements simultaneously [15, 16]. In some cases, the gaps were observed in the terahertz (THz) energy ranges.

Typically, by the THz radiation refers the high frequency electromagnetic waves with frequencies from 0.3 to 3 THz (1.2-12 meV), but some people define it as the waves with frequencies between 0.1 and 10 THz [17]. The application of quasi-metallic CNTs as the building blocks of novel high-frequency devices like the THz emitters, detectors, multipliers, antennas, polarizers, and transistors is one of the emerging trends in technology. Possibly, the most complete description of the devices and applications of such nanotubes for the THz technology are presented in the topical reviews [18 - 21]. Let us give here a few typical examples only. At a bias voltage of about 10 mV, a suspended quasi-metallic CNT of specific geometry emits light owing to Joule heating, displaying strong peaks in the THz region [22]. Using similar configuration, a temperature dependent electrically driven light emission originating from the electron-hole recombination was realized [23, 24]. In the pn-junctions fabricated using the quasi-metallic CNTs, the photocurrents are two orders of magnitude higher than those of the semiconducting nanotube devices [25]. The THz detectors based on the field-effect transistors containing only one quasi-metallic

CNT are designed, in which the single-electron excitations depending on the band structure of tubule are suggested to determine the high-frequency response [26]. The transistors with single quasi-metallic CNT have very small gate modulation with ON/OFF ratio below 100 and show ambipolar behavior, which gives certain advantages of their use in molecular electronics by comparison with transistors based on the semiconducting nanotubes [27, 28]. A bolometric response of quasi-metallic CNTs fabricated on the silicon, oxidized silicon, and sapphire substrates can be used for the THz detection and measurements [29, 30]. It is to be noted that a consensus has not been achieved on a nature of gap in the quasi-metallic CNTs [20, 21, 31]. The gaps of the same quasi-metallic CNTs on- and off-substrate differ about ten times due to the trapped charges in substrates [32]; the image charge effects on a metallic substrate affect the measured band gap of semi-conducting nanotubes [33]. It is unclear, if the single-particle or collective excitations determine the experimental gaps; using transport spectroscopy, the gaps equal to 10-100 meV were observed in all clean suspended tubules even in nominally metallic (n,n) armchair nanotubes due to the electrons interaction and formation of Mott's insulation state [20, 21, 31]. There is a discussion of a role of plasmon oscillations in the THz absorption of such tubules. The twists and axial strains produced during the fabrication of devices can result in formation of gaps in Fermi region. In the quasi-metallic CNTs, all these effects contribute to the experimental gaps together with nanotube surface curvature. The situation is also complicated by the fact that experimental studies typically employed the unidentified individual tubules or even bulk samples with statistical distribution of chiralities and diameters of the CNTs.

The zone-folding approach was fairly successful in determining the family of quasi-metallic CNTs, but it fails in predicting the exact gaps, and the first-principle calculations are necessary to study their electronic behavior. However, the standard first-principle methods applying the atomic or plane-wave basis sets and only translational symmetry are computationally quite cumbersome for calculating the chiral quasi-metallic CNTs having many hundreds and thousands atoms per translational unit cells. For this reason, there are no quantitative theoretical data on

the band structure of such tubes. We know only several nonempirical band structure calculations of zigzag quasi-metallic CNTs (n, 0) (see below).

The purpose of this work is to fix this problem, namely, using a linearized augmented cylindrical waves (LACW) method to calculate the band structure of quasi-metallic CNTs of different chirality and diameter. It is hoped that the information obtained would be useful for the identification of quasi-metallic CNTs and further progress of terahertz technology based on these tubes. The paper is organized as follows. In Section 2, avoiding the tedious algebra, which is available in our previous works, we outline the main physical ideas of the LACW technique and summarize the symmetry properties of the tubules which are very important both for the practical calculations and interpretation of the band structure. The calculated band structures together with their discussions from the point of view of possible THz applications are presented in Section 3. Section 4 provides the conclusions.

2 Methods of calculation

The LACW method is an extension of a linearized augmented plane wave (LAPW) technique [34 - 36] to the particular case of the tubular monoperiodic systems. Similar to the original APW/LAPW models, we also apply the muffin-tin and local density exchange approximations for electronic potentials, the tube being positioned between the two cylindrical barriers, which separate the multiatomic system from the vacuum regions outside and inside of tubule. The computational features of the nonrelativistic and relativistic LACW techniques, as well as their applications to the non-chiral and chiral metallic and semiconducting single-walled and double-walled carbon are described elsewhere [37 - 41], where a better determination of the electronic band gaps is achieved in comparison with other traditional methods.

The (n_1, n_2) nanotube has an axis of C_n symmetry, where n is the greatest common factor of n_1 and n_2. The nanotubes are also invariant under the screw $S(h,\omega)$ translations, which are the displacements h along the Z axis with rotations ω about it. Here, we apply the symmetry-adapted version of LACW theory applicable to any tubule independent of a number N_{Tr} of atoms in the translational

unit cell [40]. With account of rotational and screw symmetries, the unit cell is reduced to a diatomic one and the band structure of tubules can be presented in the simple form of four curves for the valence band plus curves for the low-energy states of the conduction band as the functions of the wave vector $0 \leq k \leq \pi/h$ and rotational quantum number L = 0, 1, ..., n − 1.

The main argument for using the cylindrical waves is to account for the cylindrical geometry of the nanotubes in an explicit form that, together with due account of the CNTs screw symmetry, offers the obvious advantages over application of standard plane-wave or atomic basis sets. The LACW method is the only first-principle technique permitting the calculations of any chiral nanotube.

3 Results and discussion

Let us start from the band structures of the eight small-diameter CNTs with $4 \leq n_1 \leq 8$ shown in the Figure 1. Due to the very large curvature of the surface of these tubes, the zone-folding type band structure is almost totally distorted here [42]. Particularly, the CNTs with $n_1 = 4$, 5, and 6, as well as the (7,1) tubule are the metallic ones due to an overlap of different bands. There are large curvature-induced gaps equal to the $E_g = 0.92$ eV for (4,1) CNT and 0.38 eV for the (7,1) tube, but the minimum energy points m of the conduction bands are located below the valence band tops. In the (7,4), (8,2), and (8,5) tubules with larger diameters and smaller curvature, the expected gaps equal to 0.125, 0.32, and 0.058 eV persist, but they are too large for the THz applications.

Figure 2 shows the band structures of the (9, n_2) CNTs series (n_2 = 0, 3, and 9) written in the terms of repeated zone scheme. For the (9,0) and (9,3) CNTs, the minimum energy gaps between the conduction and valence bands correspond to the points L=6, k = 0.52 a.u.$^{-1}$ ≈ $2\pi/3h$ and L=2, k = 1.88 a.u^{-1} ≈ $2\pi/3h$, respectively. In the case of (9,6) tubule, the minigap is located at k = 0.007 a.u.$^{-1}$ that is virtually at the Brillouin zone Γ point on the boundary between L=1 and L=2 regions with slight shift in the L = 2 direction. The increase in the index n_2 is accompanied by the decrease of the band gap energy E_g from 0.19 to 0.11 and 0.035 eV. The band gap narrowing agrees qualitatively with the simple π-electron theory predicting that increasing the CNT radius R and chirality angle θ should result in a reduction of the minigap [8, 21]
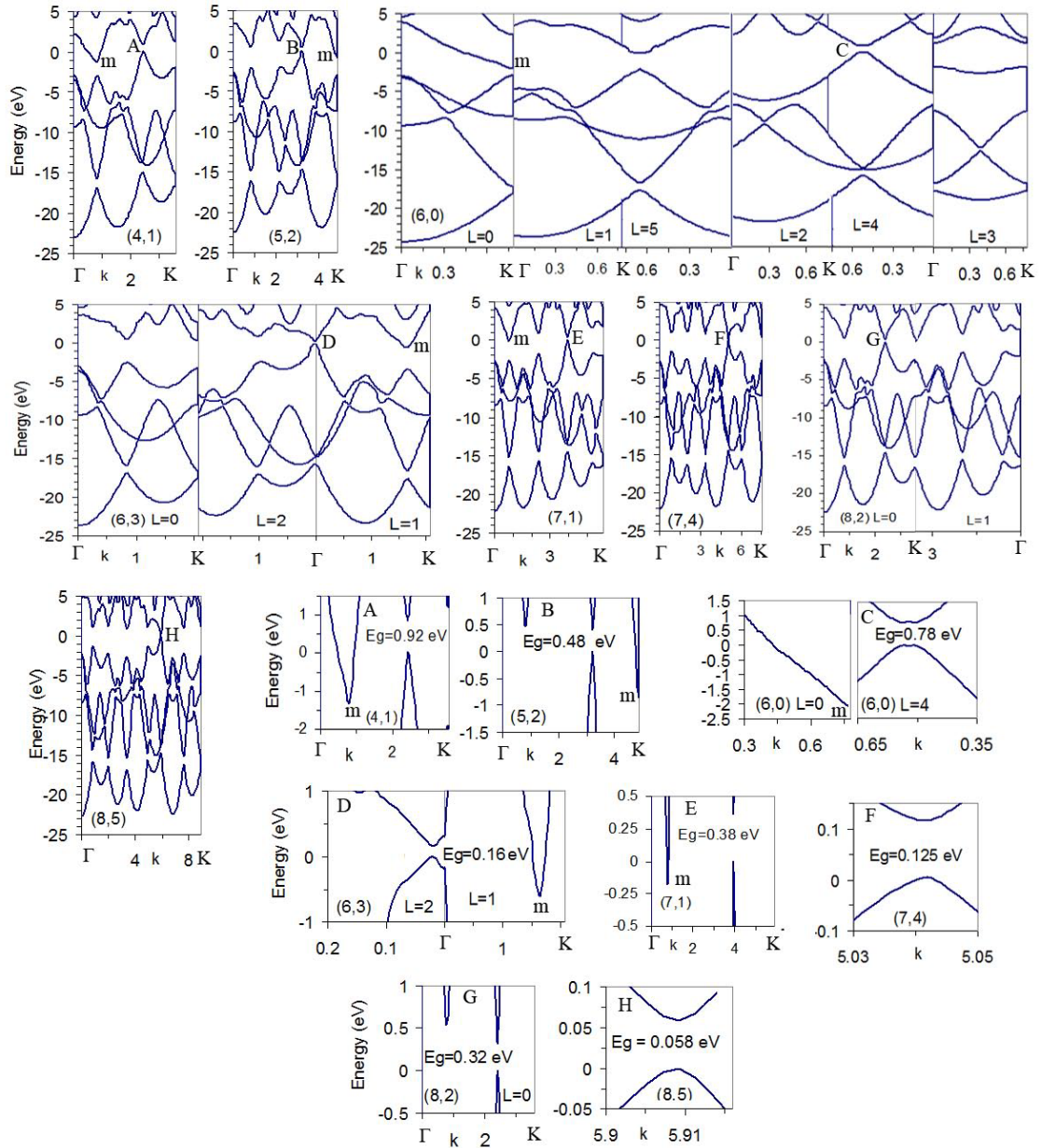
FIGURE 1 Band structures of the (n_1, n_2) CNTs with $4 \leq n_1 \leq 8$. Here and below, the energy zero is taken at the valence band top; dispersion curves in the minimum gap regions (A, B, …) are presented in enlarged energy scale; points Γ and K correspond to the $k = 0$ and $k = \pi/h$

$$E_g = \frac{\hbar v_F d_{C-C}}{8R^2} \cos 3\theta \qquad (1)$$

where $v_F = 7.25 \cdot 10^5$ m/s is the Fermi velocity of graphene. The increase of the n_2 index leads to increase of both R and θ. For the $(9, n_2)$ CNTs, the π electron E_g values are about three times underestimated compared with the LACW data, the similar significant underestimation of minigaps energies in the π electron model

is also true for majority of other nanotubes studied. Note that recent experimental data for the suspended tubules [25, 33] also show that empirical tight-binding models underestimate the gap in 3-4 times. For the (9,0) tubule, the LACW E_g = 0.19 eV value can be compared with experimental gap E_g = 0.08 eV for nanotube deposited on a gold substrate and with the following gaps obtained earlier by using a local-density approximation (LDA): 0.08[43], 0.093[44] 0.096[45], 0.17[7], 0.17[43] (LDA with
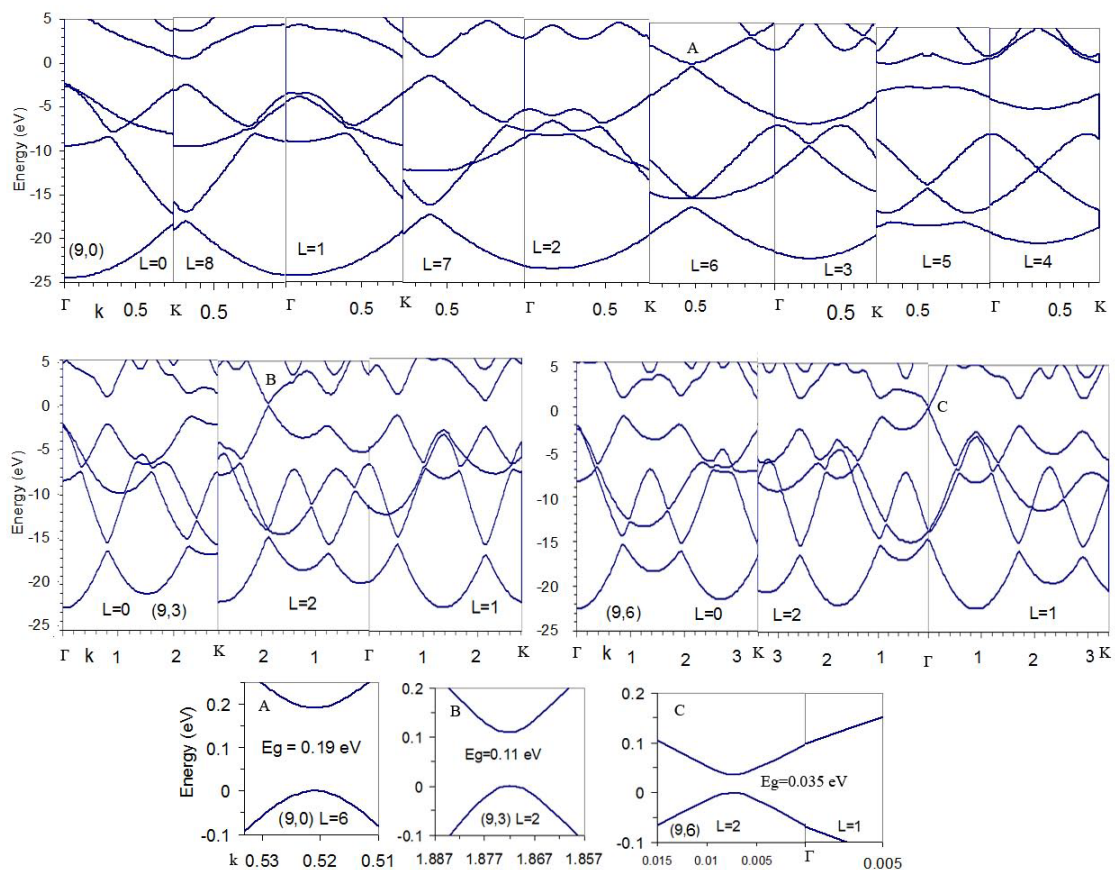
FIGURE 2 Band structures of the (9,0), (9,3), and (9,6) CNTs

many-body corrections), and 0.20 eV[46]. For the (9,3) tubule, the LACW E_g = 0.11 eV; the LDA pseudopotential gap equal to 0.02 eV appears to be much too low even from the point of view of the π electron theory [47].

The transition from zigzag (9,0) CNT with 9th order rotational axis to the low-symmetry chiral (10,1) tubule is accompanied by dramatic simplification of band structure, but it almost does not affect the band gap. The same is true for the pairs (9,3) and (10,4), (9,6) and (10,7) (Figure 3). In the (10,1) and (10,7) CNTs with C_1 axis, the gaps are located at k ≈ 2π/3h; in the case of (10,4) tubule with C_2 rotational symmetry, the gap is near the k ≈ 2π/3h point for the L = 0.

There is no rotational symmetry in the CNTs (11, n_2) with n_2 = 2, 5, and 8. The gaps are located near k = 2π/3h for L = 0 in all cases (Figure 4). The nanotubes radii and chirality angles of these tubules are noticeably larger than those of the corresponding (9, n_2) CNTs, and the gaps of the (11, n_2) tubes are about 30 per cent smaller. Among the nine (9, n_2), (10,n_2), and (11, n_2) CNTs, the E_g values are less than 0.040 eV, i.e., the optical gap are in

the THz region only in the case of the three tubes (9,6), (10,7), and (11,8) the largest R and θ values. In these three series, the gaps decrease approximately linearly as functions of the n_2 index. In literature, there are no experimental or ab initio data on the band structure and gap energies for these chiral tubules.

In contrast to the naive π electron model, according to which the growth of the index n_2 must always lead to a narrowing of the gap, the LACW method predicts that the dependence of E_g on the n_2 is nonmonotonic among the nanotubes (12, n_2) with n_2 = 0, 3, 6, and 9 (Figure 5). The maximum forbidden gaps E_g = 0.076 and 0.077 eV are observed for n_2 = 3 and 6; they are almost two times larger than the gap equal to 0.042 eV for the tube (12,0). The gaps are near the point k = 2π/3h for L = 8 and L = 0 in the case of the (12,0) and (12,3) CNTs, respectively, and are near Brillouin zone center k = 0 in the boundary between L = 2, L = 4 and L = 2, L = 1 regions in the case of the (12,6) and (12,9) CNTs, respectively. Again only one tubule (12,9) with E_g = 0.013 eV falls in the THz range. The LACW energy gap coincides
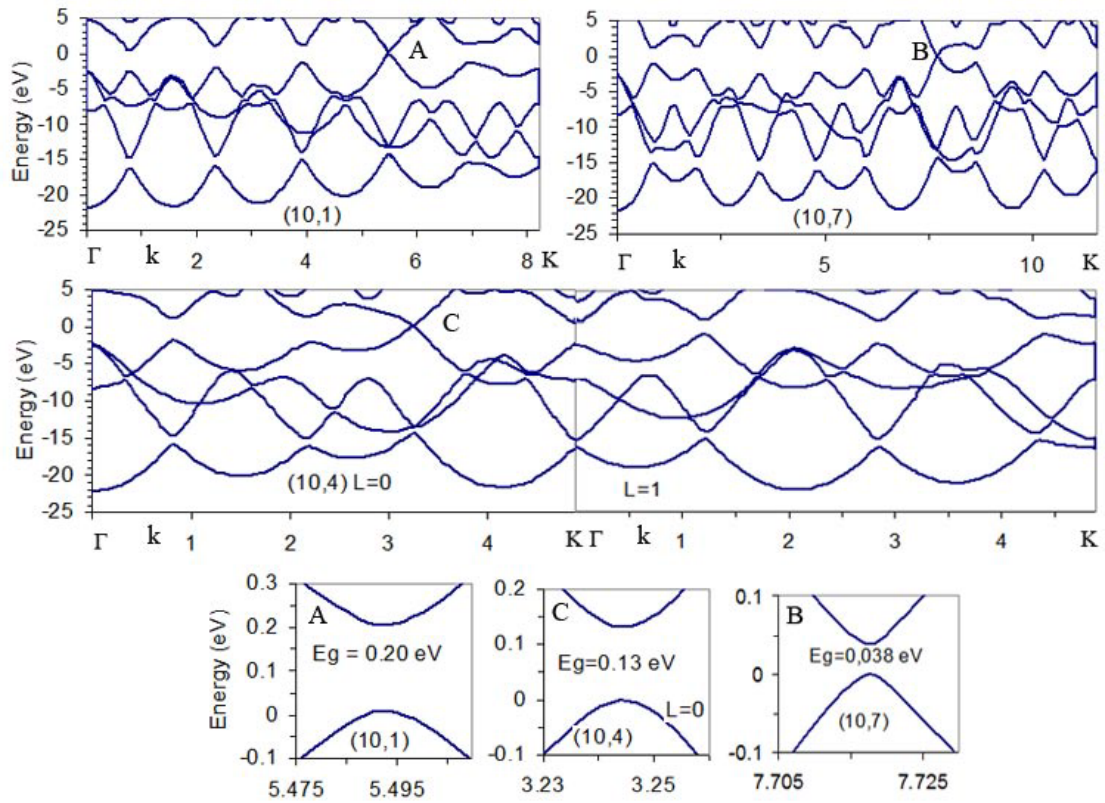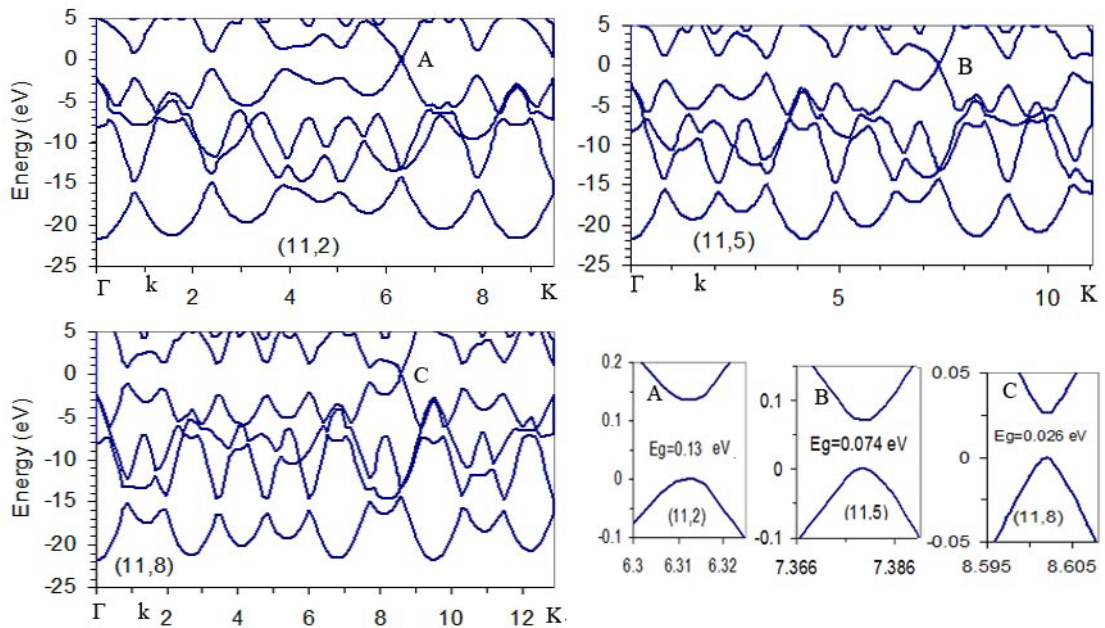
FIGURE 3 Band structures of the (10, n2) CNTs

FIGURE 4 Band structures of the (11, n₂) CNTs

with experimental value E_g = 0.042 eV for the (12,0) nanotube deposited on a gold substrate [11], and can be compared with the values of 0.040, 0.078, and 0.08 eV obtained using LDA calculations [44 - 46].

According to the equation (1), the transition from the (12,0) tube to the (13,1) and (14,2) CNTs should be accompanied by a decrease of E_g. However, instead, the LACW method shows the threefold gap increase up to 0.14 and 0.13 eV, respectively. To best of our knowledge, the (13,1) CNT is the only chiral tubule, for which the experimental gap was identified and shown to be equal to the 0.18 eV using the device with suspended the CNT [48]. Figures 6 and 7 show that the LACW band gaps decrease monotonically with increasing n_2 index in the series (13, n_2) with n_2 = 1, 4, 7, 10 and (14, n_2) with n_2 = 2, 5, 8, 11 in

accordance with equation (1). Only the (13,10) and (14,11) CNTs with the maximum n_2 values and, therefore, minimum gaps equal to 0.015 and 0.011 eV are in the THz frequency range.

Similar to the case of (12, n_2) CNTs and in contrast to the predictions of π electron model, the gap width increases from 0.022 to 0.050 eV at the transition from the zigzag tube (15,0) to the chiral tube (15,3) (Figure 8). Further increase of the n_2 index in the (15, n_2) series results in the gap decrease down to a value of 0.029, 0.015, and 0.006 eV for the (15,6), (15,9), and (15,12) tubules, respectively. The gaps correspond to the Brillouin zone points k ≈ $2\pi/3_h$ for the CNTs (15,0) (L = 10), (15,6) (L = 0), (15,9) (L = 2), or to the Γ point separating L = 2 and L = 1 regions in the case of (15,3) and (15,12) CNTs. Only for the (15,0) CNT, the LACW E_g = 0.022 eV can be

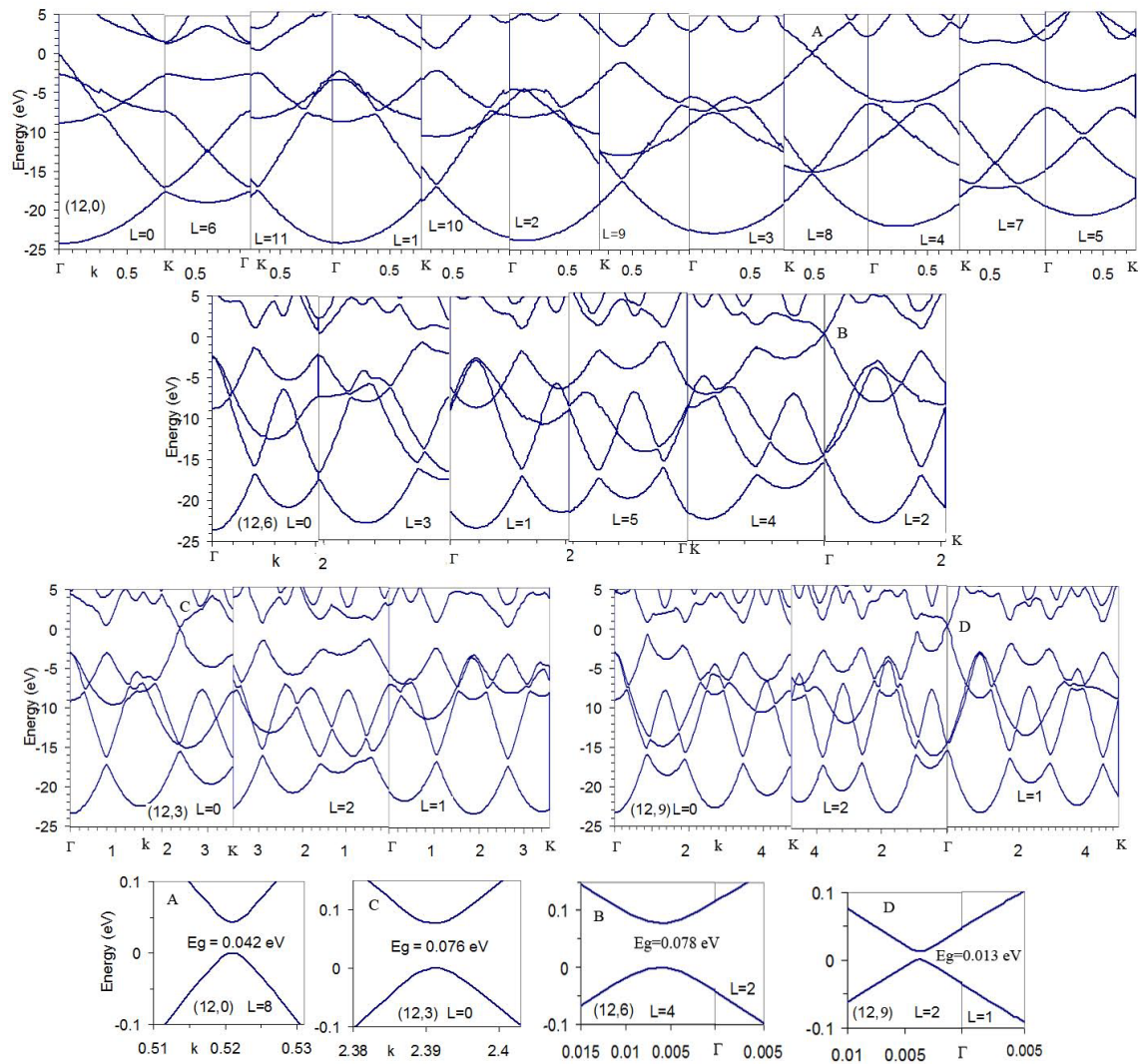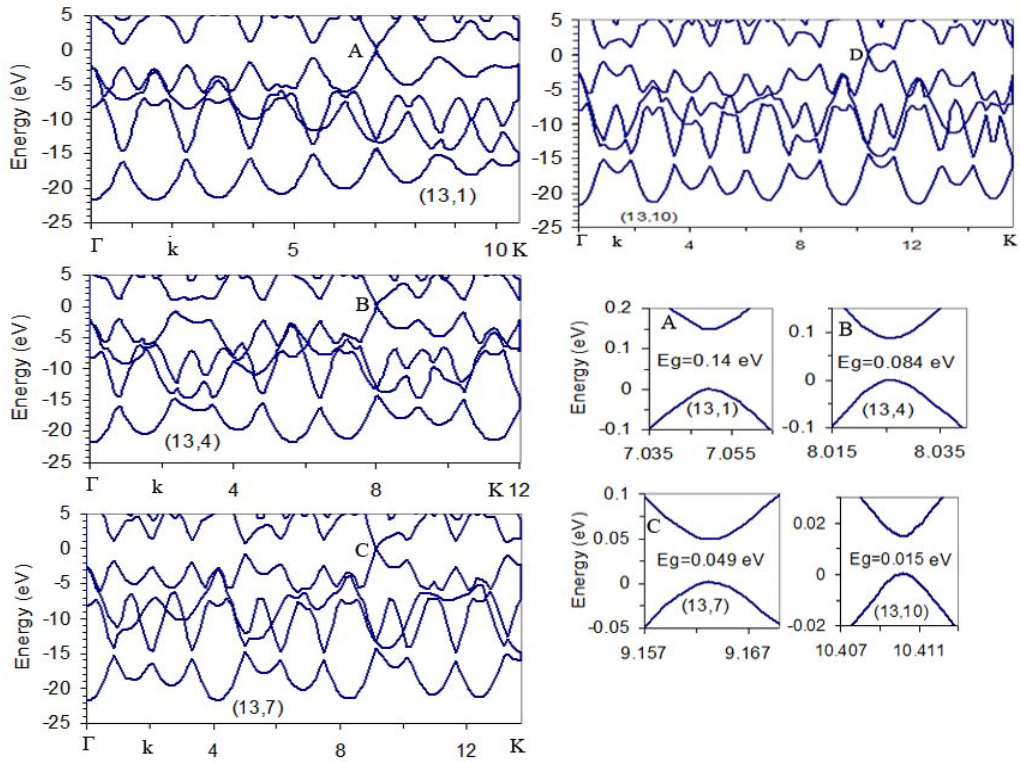

FIGURE 5 Band structures of the (12, n2) CNTs

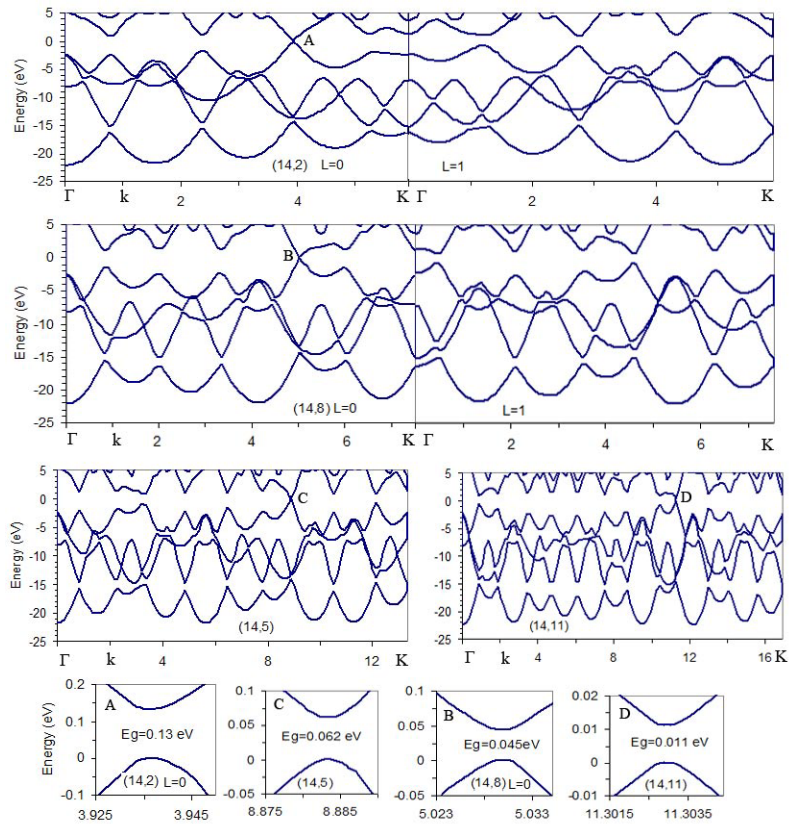FIGURE 6 Band structures of the (13, n2) CNTs

FIGURE 7 Band structures of the (14, n2) CNTs

compared the experimental gap equal to 0.029 eV [11] for the tube on Au substrate and with following LDA data: 0.023 [45], 0.028 [44], and 0.030 eV [46].

Figures 9 and 10 show that the gaps of (16, n_2) and (17, n_2) CNTs are larger than those of the (15, n_2) counterparts in the case of small n_2 indices; as expected, increasing n_2 is accompanied by the reduction of gaps. About half of these tubes have the gap in the THz region.

In the (18, n_2) CNTs, the gaps range from the 0.003 to 0.038 eV, that is, they all are in the THz region. With the growth of n_2 index, initially the gap increases from the E_g = 0.009 eV to the E_g = 0.030-0.038 eV and then drops to the value equal to the 0.003 eV for n_2 = 15 (Figure 11).

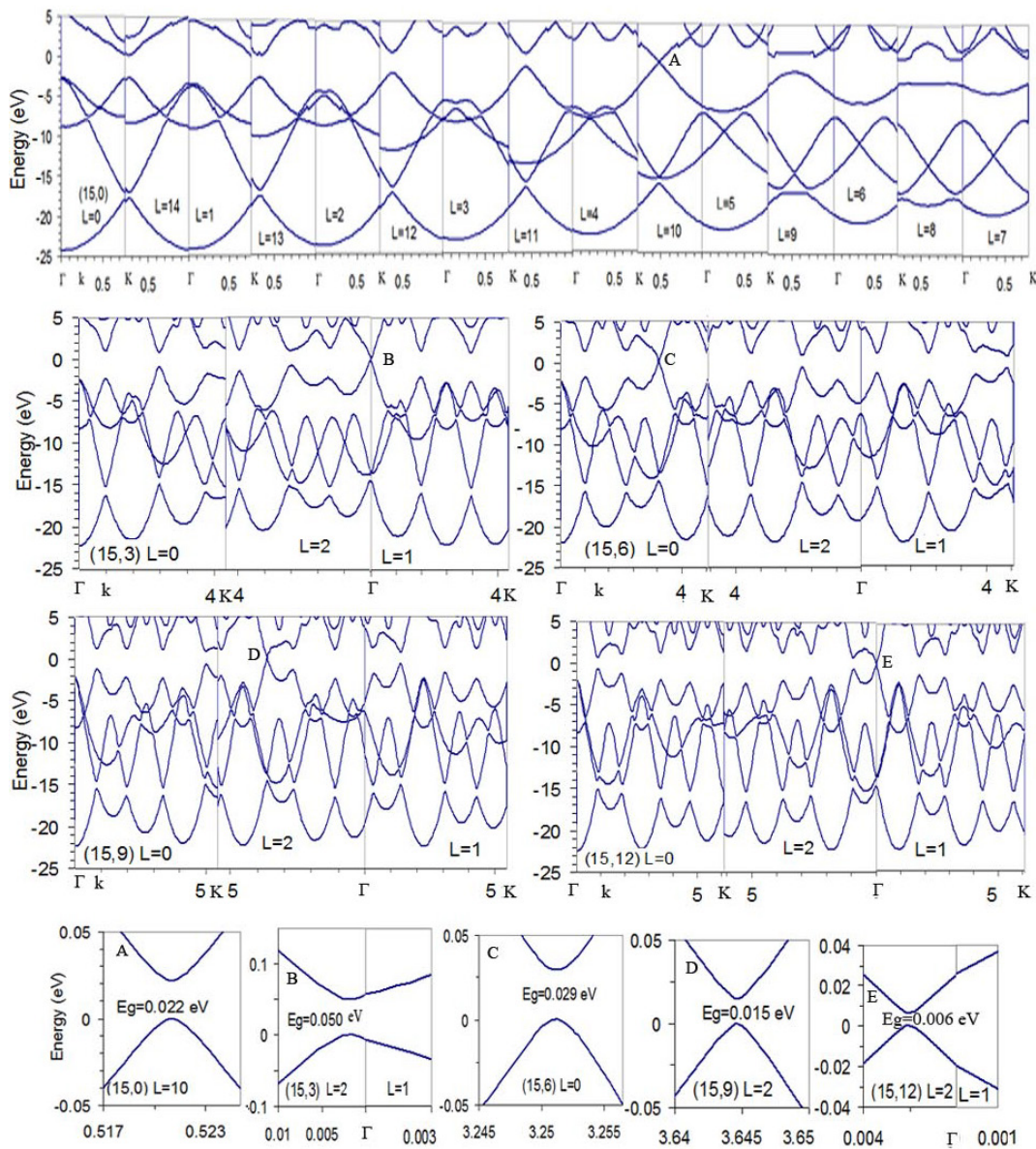Figure 12 shows plots, where the trends in E_g versus the CNTs radii and chirality can be easily followed.
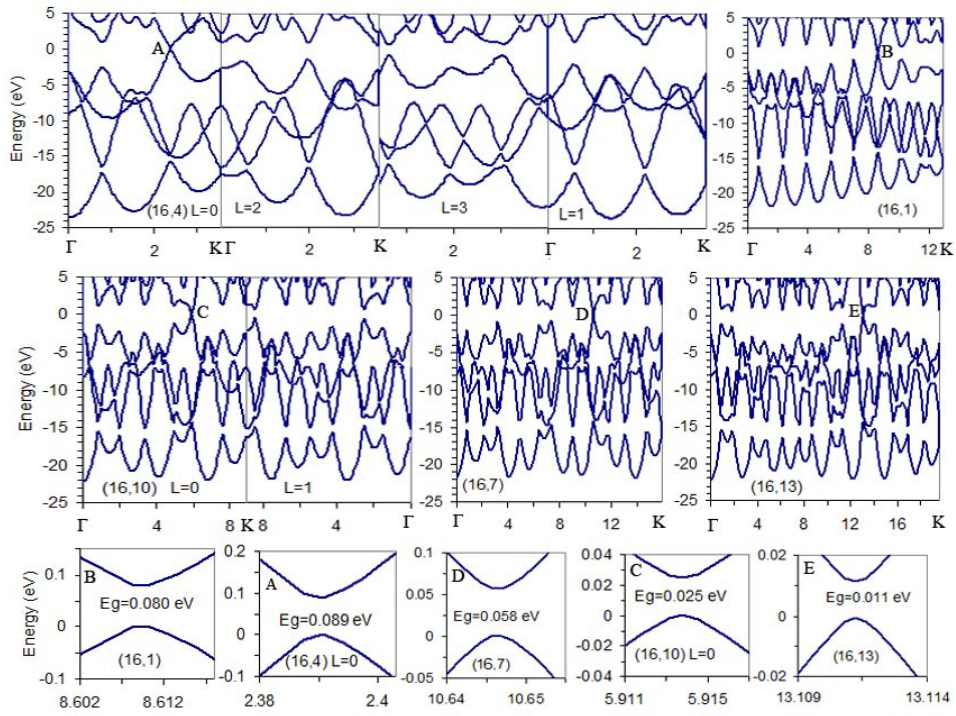

FIGURE 8 Band structures of the (15,n_2) CNTs
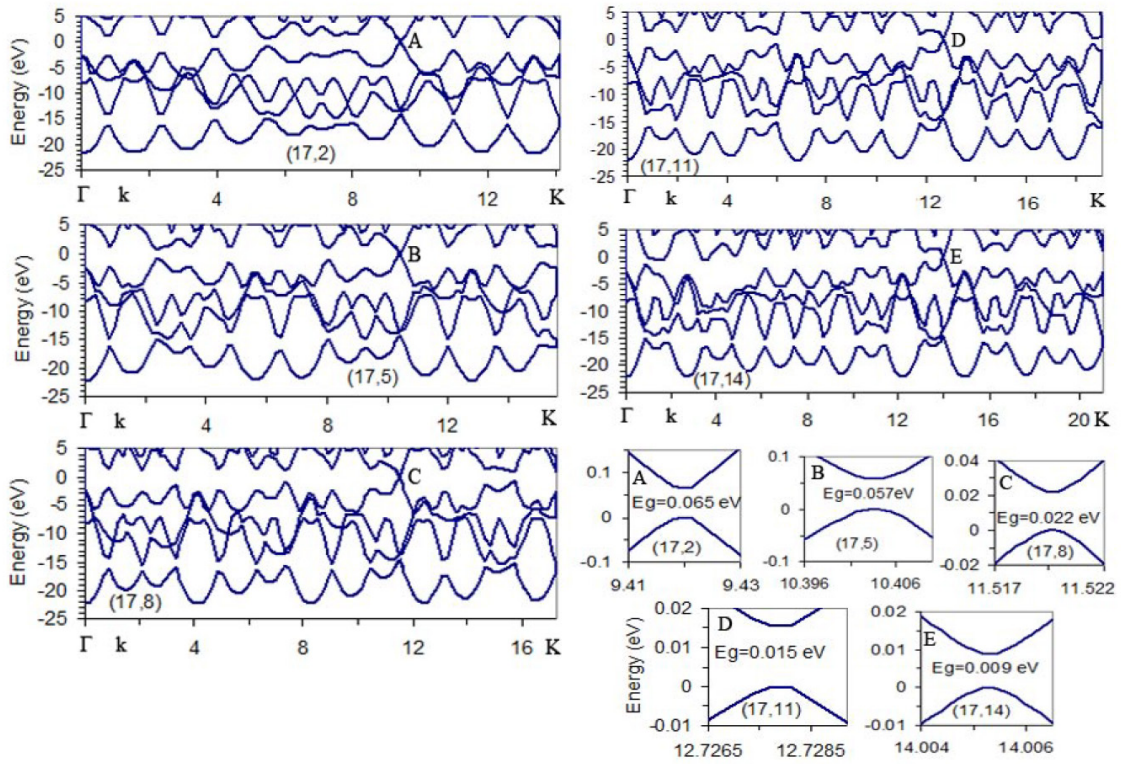
FIGURE 9 Band structures of the (16, n2) CNTs
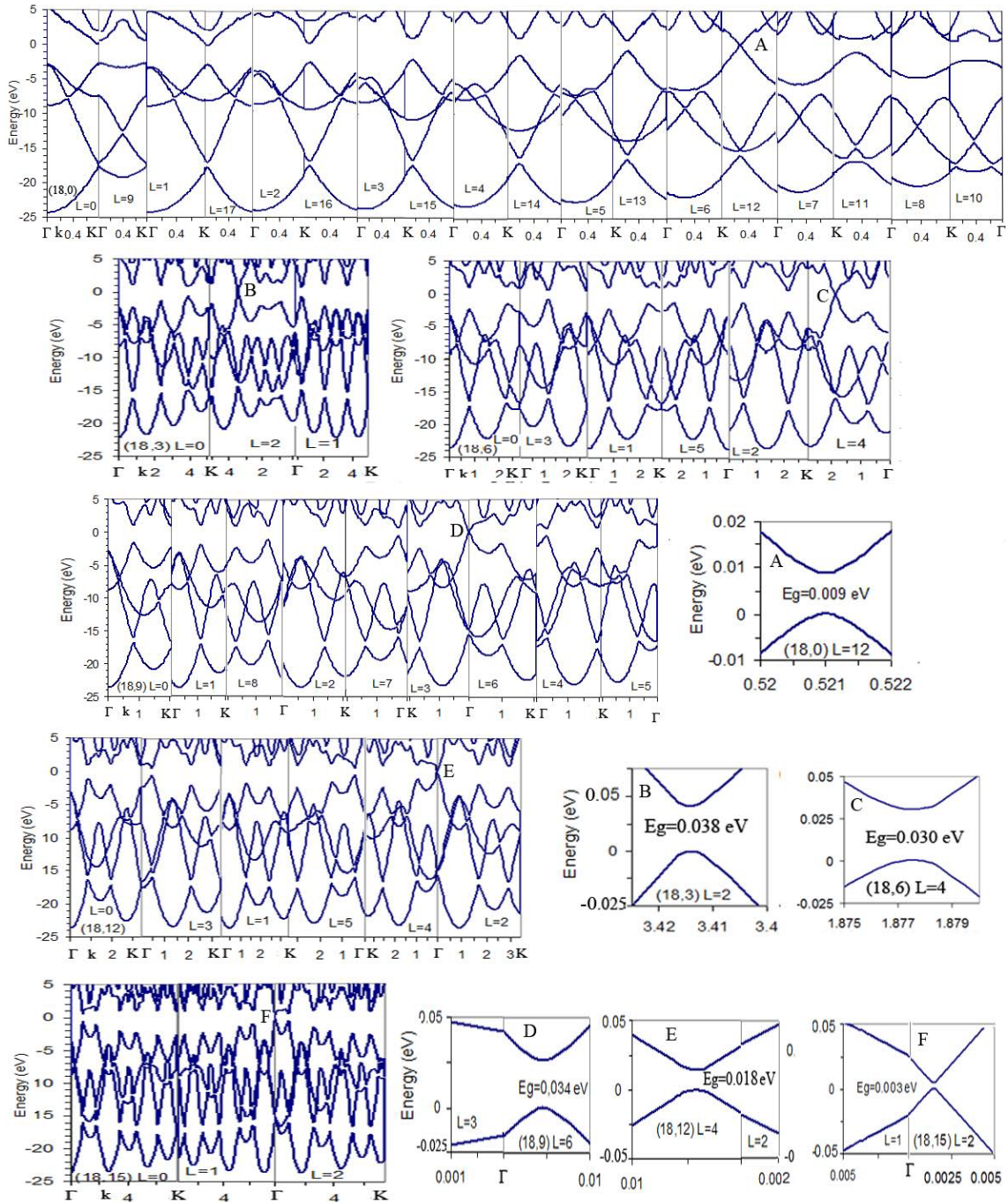
FIGURE 10 Band structures of the (17, n₂) CNTs
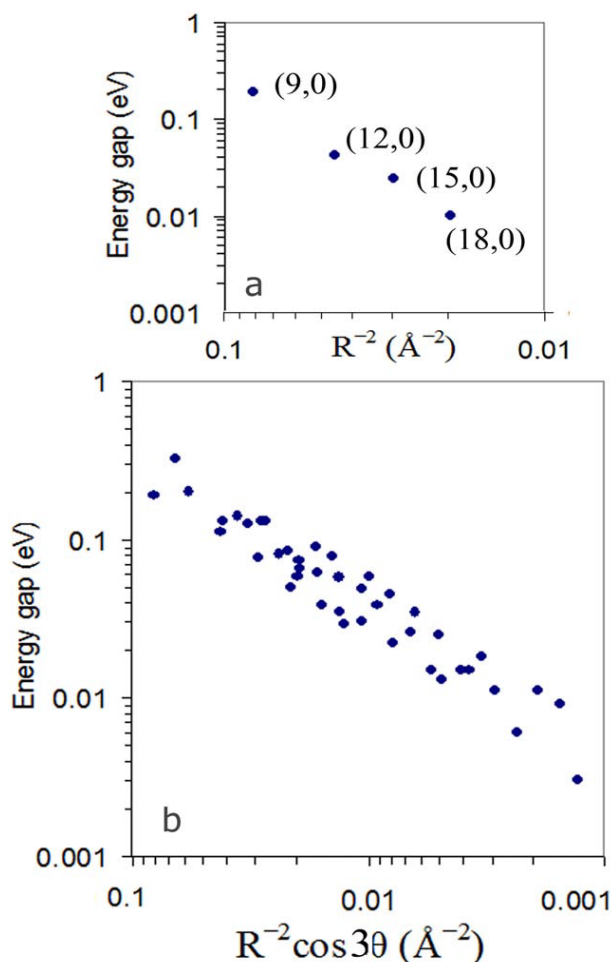
FIGURE 11 Band structures of the (18, n₂) CNTs

FIGURE 12 The trends in Eg versus the CNTs radii and chirality. (a) zigzag CNTs; (b) chiral CNTs

4 Conclusions

The linearized augmented cylindrical wave method has been used to study the band structures of the 50 different both chiral and zig-zag single-walled carbon nanotubes (n_1, n_2) with ($n_1 - n_2$)mod3 = 0. In the Fermi energy region, the formation of energy gaps depending on the tubules geometry is obtained. The

nanotubes with optical gaps falling within the THz range are identified. These findings can be of great importance for application of nanotubes in the nanoelectonic THz devices.

Acknowledgments

References

[1] Hamada N, Sawada S I, Oshiyama A 1992 *Phys. Rev. Lett.* **68** 1579

[2] Saito R, Fujita M, Dresselhaus G, Dresselhaus M S 1992 *Phys. Rev.* **B 46** 1804

[3] Saito R, Fujita M, Dresselhaus G, Dresselhaus M S 1992 *Appl. Phys. Lett.* **60** 2204

[4] White C T, Robertson D H, Mintmire J W 1993 *Phys. Rev.* **B 47** 5485

[5] Dresselhaus M S, Dresslhaus G, Saito R 1995 *Carbon* **33** 883

[6] Mintmire J W, Robertson D H, White C T 1993 *J. Phys.*

Chem. Solids **54** 1835

[7] Blase X, Benedict L X, Shirley E L, Louie S G 1994 *Phys. Rev. Lett.* **72** 1878

[8] Kane C L, Mele E J 1997 *Phys. Rev. Lett.* **78** 1932

[9] Chibotaru L F, Bovin S A, Ceulemans A 2002 *Phys. Rev.* **B 66** 161401(R)

[10] Hartmann R R, Portnoi M E 2015 *IOP Conf. Series: Materials Science and Engineering* **79** 012014

[11] Ouyang M, Huang J L, Cheung C L, Lieber C M 2001 *Science* **292** 702

[12] Itkis M E, Niyogi S, Meng M E, Hamon M A, Hu H,

Haddon R C 2002 *Nano Letters* **2** 155

[13] Borondocs F, Kamarás K, Nikolou M, Tanner D B, Chen Z H, Rinzler A G 2006 *Phys. Rev.* **B 74** 045431

[14] Pekker A, Kamara K 2011 *Phys. Rev.* **B 84** 075475

[15] Kampfrath T, von Volkmann K, Aguirre C M, Desjardins P, Martel R, Krenz M, Frischkorn C, Wolf M, Perfetti L 2008 *Phys. Rev. Lett.* **101** 267403

[16] Bushmaker A W, Deshpande V V, Hsieh S, Bockrath M W, Cronin S B 2009 *Phys. Rev. Lett.* **103** 067401

[17] Mantsch H H, Naumann D, Molec J 2010 *Struct.* **964** 1

[18] Nemilentsau A M, Slepyan G Y, Maksimenko S A, Kibis O V, Portnoi M E 2010 *The Handbook of nanophysics Vol 4. Nanotubes and nanowires* Edited by Edited by Klaus D. Sattler **Chapter 5** 1

[19] Hartmann R R, Portnoi M E 2016 *AIP Conf. Proc.* **1705** 020046

[20] Portnoi M E, Kibis O V, da Costa M R 2008 *Superlattices and Microstructures* **43** 399

[21] Hartmann R R, Kono J, Portnoi M E 2014 *Nanotechnology* **25** 322001

[22] Mann D, Kato Y K, Kinkhabwala A, Pop E, Cao J, Wang X 2007 *Nature Nanotechnology* **2** 33

[23] Mueller T, Kinoshita M, Steiner M, Perebeinos V, Bol A A, Farmer D B 2010 *Nature Nanotechnology* **5** 27

[24] Wang X, Zhang L, Lu Y, Daia H, Kato Y K, Pop E 2007 *Appl. Phys. Lett.* **91** 261102

[25] Chang S-W, Hazra J, Amer M, Kapadia R, Cronin S B 2015 *ACS Nano* **9** 11551

[26] Zhong Z, Gabor N M, Sharping J E, Gaeta A L, McEuen P L 2008 *Nature Nanotechnology* **3** 201-5

[27] Cui X, Freitag M, Martel R, Brus L, Avouris P 2003 *Nano Lett.* **3** 783

[28] Choi S 2014 *Efficient antennas for terahertz and optical frequencies* A dissertation University of Michigan

[29] Santavicca D F, Prober D E 2008 *33rd Intern. Conf. on Infrared, Millimeter and terahertz Waves. IEEE, Pasadena, CA*

[30] Fu K, Zannoni R, Chan C, Adams S H, Nicholson J, Polizzi E, Yngvesson K S 2008 *Appl. Phys. Lett.* **92** 033105

[31] Deshpande V V, Chandra B, Caldwell R, Novikov D S, Hone J, Bockrath M 2009 *Science* **323** 206

[32] Amer M R, Bushmaker A, Cronin S B 2012 *Nano Lett.* **12** 4843

[33] Lin H, Lagoute J, Repain V, Chacon C, Girard Y, Lauret J S, Ducastelle F 2010 *Nature Materials* **9** 235

[34] Slater J C 1937 *Phys. Rev.* **51** 851

[35] Andersen O K 1975 *Phys. Rev.* **B 12** 3060

[36] Koelling D D, Arbman G O 1975 *J. Phys. F: Met. Phys.* **5** 2041

[37] D'yachkov P N 2016 *Intern. J. Quantum Chem.* **116** 174

[38] D'yachkov P N, Makaev D V 2016 *Intern. J. Quantum Chem.* **116** 316

[39] D'yachkov P N, Kutlubaev D Z, Makaev D V 2010 *Phys. Rev.* **B 82** 035426

[40] D'yachkov P N, Makaev D V 2007 *Phys. Rev.* **B 76** 195411

[41] D'yachkov P N, Hermann H, Kirin D V 2002 *Appl. Phys. Lett.* **81** 5228

[42] D'yachkov P N, Hermann H 2004 *J. Appl. Phys.* **95** 399

[43] Miyake T, Saito S 2005 *Phys. Rev.* **B 72** 073404

[44] Gülseren O, Yildirim T, Ciraci S 2002 *Phys. Rev.* **B 65** 153405

[45] Zólyomi V, Kürti J 2004 *Phys. Rev.* **B 70**, 085403

[46] Sun G, Kürti J, Kertesz M, Baughman R H 2003 *J. Phys. Chem.* **B 107** 6924

[47] Reich S., Thomsen C, Ordejón P 2002 *Phys. Rev.* **B 65** 155411

[48] Amer M R, Chang S-W, Dhall R, Qiu J, Cronin S B 2013 *Nano Lett.* **13** 5129

AUTHORS

Pavel D'yachkov, 2 December 1947, Saint Petersburg (the former Leningrad), Russia

Current position, grades: Prof. Dr., Principal Investigator, Quantum Chemistry Laboratory, Kurnakov Institute of General and Inorganic Chemistry
University studies: Moscow and Leningrad Universities, Chemistry Departments
Scientific interest: Quantum Chemistry of Inorganic, Coordination, and Nanomaterials
Publications: Author of about 150 journal papers and five books including "Heteroligand Molecules: Structure, Isomers, Transformations" (Francis and Taylor, London and New York, 2002, 271 p; with Alexander A. Levin).
Experience: Theoretical and Computational Chemistry

Ilya Bochkov, 26 February 1989, Ryazan, Russia

Current position, grades: Private company, Engineer
University studies: Ryazan State Radiotechnical University, Ryazan, Russia; Industrial Electronics Engineer, Student, PhD student
Scientific interest: Computational Chemistry, Nanomaterials
Publications: 17 journal papers
Experience: Computational material science